Solar Energy Materials and Solar Cells 185 (2018) 153–157

Contents lists available at ScienceDirect

Solar Energy Materials and Solar Cells

journal homepage: www.elsevier.com/locate/solmat

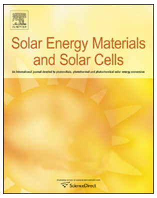

Epitaxial Lift-off (ELO) of InGaP/GaAs/InGaAs solar cells with quantum dots in GaAs middle sub-cell

Sudersena Rao Tatavarti[a,*,1], Zachary S. Bittner[b,1], A. Wibowo[a], Michael A. Slocum[b], George Nelson[b], Hyun Kum[b], S. Phillip Ahrenkiel[c], Seth M. Hubbard[b]

[a] *MicroLink Devices, 6457 Howard Street, Niles, IL, USA*
[b] *Rochester Institute of Technology, Rochester, NY, USA*
[c] *South Dakota School of Mines and Technology, Rapid City, SD, USA*

ARTICLE INFO

Keywords:
Inverted metamorphic (IMM)
Solar cells
Quantum dots (QD's)
Radiation hard
Multijunctions
MOCVD
Epitaxial Lift-off (ELO)

ABSTRACT

We report the first demonstration of MOVPE-grown inverted metamorphic (IMM) cells with QDs embedded in the middle GaAs sub-cell. The IMM cells were fabricated on full 4″ wafer using Epitaxial Lift off (ELO) technology. GaAs sub-cell embedded with 10 and 20 periods of InAs/GaP strain compensated QDs showed increase in current with number of QD periods. The single junction GaAs sub cell embedded with 20 periods of InAs/GaP strain compensated QDs showed 3.2% relative increase in J_{SC} in comparison with control sample without QDs. Integrated short circuit (J_{SC}) from measurements of external quantum efficiency (EQE) of currents showed a 65% increase in sub-band collection in the GaAs sub-cell when the number of QD layers increased from 10 to 20. IMM cells with QD's embedded in the middle cell showed minimal loss in open circuit voltage (V_{OC}) in comparison to control sample without QDs. An efficiency of 30% under 1-sun AM0 spectrum was obtained for IMM cells with 10 xs of InAs/GaP QDs in GaAs sub-cell. Quantum efficiency remaining factor of > 95% in the QD absorption region (940 nm) was measured for IMM devices with InAs/GaAs QD enhanced GaAs sub-cells irradiated with 1 MeV electrons under 2E15 /cm^2 fluence.

1. Introduction

Future space exploration missions such as the planned Europa Jupiter System Mission, and continued lunar and Mars exploration missions, require higher efficiency solar cells to reduce solar array mass, volume, and mission cost [1]. Unlike terrestrial applications, space photovoltaics continuously lose power over the course of the mission due to radiation environments in space. Thus, the development of photovoltaic devices for space is ultimately focused on maximizing specific power and minimizing areal density (kg/m^2) both at beginning and end of the mission life. Unfortunately, it is currently not possible to realize high (> 1000 W/kg) specific power at end of life (EOL) at the panel level. Panel-level mass specific power using traditional upright (30% efficient with a Ge substrate) photovoltaics is limited to ~200 W/kg [2]. Direct substitution of the inverted metamorphic (IMM) solar cells increases the panel-level specific power to only ~350 W/kg. The reason for this moderate increase in the specific power is due to the extra shielding that is needed to prevent IMM degradation due to radiation in space (mainly protons and electrons in the MeV range). An alternate method of increasing EOL mass specific power is addressing radiation tolerance using nanostructures [3].

InAs/GaAs quantum dots (QDs) have been demonstrated to improve remaining maximum power (P_{MAX}) at EOL primarily by reducing degradation of I_{SC} [3] in Ge-based triple junction solar cells. QDs also behave as efficient radiative recombination centers even as the surrounding material is degraded by alpha particle exposure [4], a characteristic that could further enhance radiation tolerance by enabling EOL luminescent coupling between sub-cells in a tandem cell [5,6].

InAs/GaAs QDs nucleate via the Stranski-Krastinov (SK) growth mode due to the lattice mismatch between InAs and GaAs [7,8]. A QD superlattice is strain balanced by the addition of tensile GaP spacer layers [7,10] or GaAsP [8,9] leading to low global strain, allowing for dislocation-free epitaxy. One theory for the increased radiation tolerance of QD-containing material is due to localized compressive strain fields emanating from the QDs [3,10] and leading to an increase in threshold energy for atomic displacement to occur.

In this work, we report results on QD-enhanced triple-junction IMM solar cells fabricated using epitaxial lift-off (ELO) [12,13] in a process

---

[*] Corresponding author.
E-mail address: rtatavarti@mldevices.com (S.R. Tatavarti).
[1] These authors contributed equally.

https://doi.org/10.1016/j.solmat.2018.05.016
Received 6 November 2017; Received in revised form 11 April 2018; Accepted 7 May 2018
0927-0248/

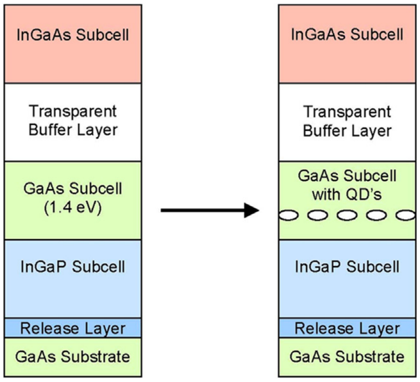

Fig. 1. IMM cell on GaAs substrate with and without QDs in the GaAs sub cell are shown.

compatible with large area 4″ and 6″ wafers. IMM InGaP/GaAs/InGaAs sub-cells with and without QDs in the middle GaAs cell were grown on GaAs substrates using metalorganic chemical vapor deposition (MOCVD). ELO technology was employed to remove the tandem cells from the GaAs substrate and transfer onto flexible, lightweight metal substrates. Incorporating 10 layers of strain compensated InAs QDs into the GaAs middle cell resulted in a 0.42 mA/cm^2 increase in short circuit current density (J_{SC}) with minimal open circuit voltage (V_{OC}) loss. The resultant IMM device with QDs showed an efficiency of 30% under 1-sun AMO with a V_{OC} of 2.90 V and J_{SC} of 16.86 mA/cm^2.

2. Experimental

The InGaP/GaAs/InGaAs metamorphic solar cells were grown by MOCVD. Fig. 1 shows the entire growth sequence of the IMM cell. ELO templates on GaAs substrates with pre-grown InGaP top cell, tunnel junction, GaAs middle cell window and partially into the middle cell emitter were sent from Microlink Devices (MLD) to Rochester Institute of Technology (RIT). Subsequently RIT grew the middle GaAs sub-cell, starting in the cell emitter, with varying (10 and 20) periods of QDs in an Aixtron Close Couple Showerhead (CCS) MOCVD reactor. Several growths were performed to optimize QD density and size on GaAs 6° off-cut substrates.

All the overgrowth on the MicroLink ELO templates used RIT's standard QD growth conditions (430 °C QD growth temperature, 1.76 ML of InAs deposition and 4 ML GaP strain balancing layer). Growth at RIT terminated in a GaAs cap after the GaAs sub-cell BSF.

Samples were then sent back to MLD for growth [12,13] of the final metamorphic buffer and $In_{0.3}Ga_{0.7}As$ bottom cell. Next the wafers went through an ELO process and solar cell device fabrication at MLD. The devices in this study were designed with a GaAs middle cell of 100 nm n$^+$ emitter and a 3.5 μm p-base, and the unintentionally doped (*uid*) region for the control and 10 QD layer structure was 180 nm while the *uid* region for the 20 QD layer structure was 300 nm.

Bi-layer ARC using MgF_2/ZnS was employed on the completed devices. One-sun AM0 IV measurements were performed on a two-zone TS Space Systems solar simulator at a cell temperature of 25 °C and irradiance of 136.6 mW/cm^2. Calibration was performed with InGaP and (In)GaAs secondary standards. Spectral response (SR) was measured using an IQE200 monochromator with a Stanford Research SR570 preamplifier and SR830 lock-in amplifier along with 470 nm, 750 nm, and 960 nm LEDs for light biasing the top, middle, and bottom cells respectively.

3. Results and discussions

Atomic force microscope (AFM) analysis, performed on a Veeco Dimension 3000 scanning probe microscope system, shown in Fig. 2, was performed on an AFM test structure grown with uncapped surface QDs to determine the density and size. Growth conditions for the surface QDs were the same as for QDs in the buried superlattices but growth was halted after QD formation leaving an uncapped layer of surface QDs. An AFM statistical analysis determined average QD densities of ~2.81 × 10^{10} cm^{-2} and average height and diameter of 2.11 nm and 20.9 nm.

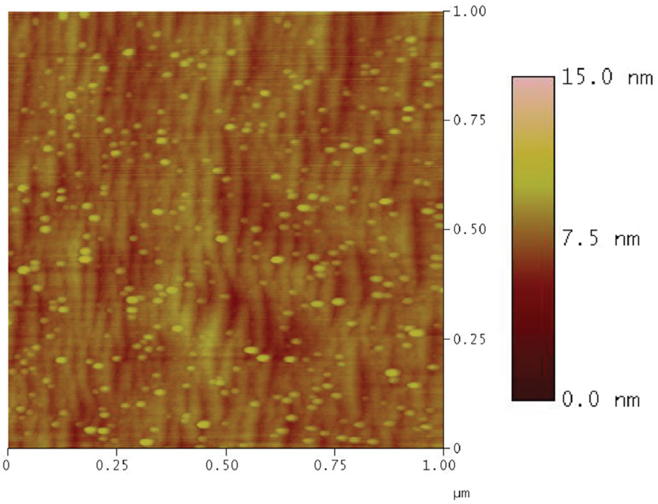

Fig. 2. AFM scans of QDs grown on MLD ELO templates.

One-sun AM0 IV results are shown in Fig. 3. The first thing to note is that the addition of 10 layers of QDs resulted in an increase in J_{SC}. The increase of ~500 μA/cm^2 (uncertainty of ± 250 μA/cm2 due to bulk and QD current generation) between control and 10 × QDSC corresponds with the increase in sub-band absorption seen in the external quantum efficiency (EQE) plot (Fig. 5). Further enhancement in J_{SC} was not observed as we increased the QD periods from 10 to 20. This may be because of the increased onset of defects in the QDs as the number of periods increased. We are currently working on increasing the QDs number further to 30 or more periods to see the changes in J_{sc}. The V_{OC} of the control device was 2.92 V, with minimal drop to 2.90 V and 2.89 V for the 10 × and 20 × QDSCs respectively, resulting in a relative efficiency enhancement of 1.3% from 29.9% to 30.3%. Fill factor has a slight reduction, which is on the order of measurement uncertainty.

The EQE of the IMM ELO cells is shown in Fig. 4. The top cells for each solar cell were grown simultaneously, as a result negligible changes in top cell performances are seen in the EQE spectrum. The

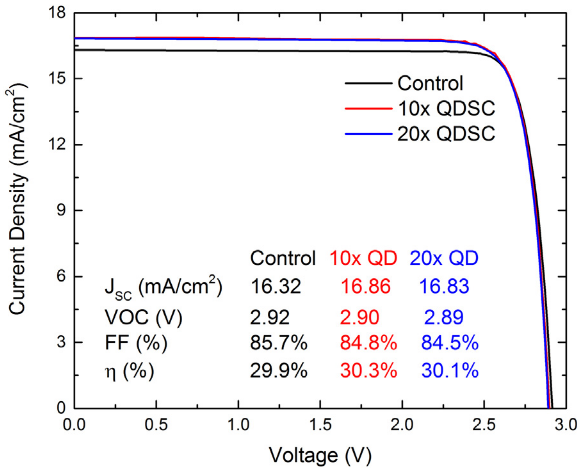

Fig. 3. One sun AM0 IV measurements for IMM ELO cells with and without QDs in the middle GaAs cell are shown.